applied sciences

MDPI

Article

Influence of Fiber Mixing Process on the Cracking Resistance of Cold Recycled Asphalt Mixture

Ming Wang [1], Tongde Huo [1], Chengwei Xing [2,3,*] and Yuxuan Wang [1]

[1] College of Transportation Science and Engineering, Civil Aviation University of China, Tianjin 300300, China
[2] Key Laboratory for Special Area Highway Engineering of Ministry of Education, Chang'an University, South 2nd Ring Road Middle Section, Xi'an 710064, China
[3] School of Highway, Chang'an University, South 2nd Ring Road Middle Section, Xi'an 710064, China
* Correspondence: xingcw@chd.edu.cn

Abstract: Fiber reinforcement is often used to improve the road performance of cold recycled asphalt mixture (CRAM). The purpose of this research is to evaluate the impact of fiber mixing process on the cracking resistance of CRAM from multiple perspectives. Four kinds of fiber mixing processes, named A, B, C, and D, were designed by changing the order of fiber addition during the mixing process. Then, semicircle bending tests and indirect tensile tests were conducted to characterize the low-temperature cracking behavior of fiber CRAM. Freeze–thaw cycle tests under both dry and water-saturated conditions were performed to investigate the freeze–thaw damage behavior of fiber CRAM. Furthermore, the fiber dispersion in CRAM was observed using scanning electron microscopy (SEM). The results show that the fiber mixing process has a significant effect on the cracking resistance of CRAM. The CRAM specimens prepared by process C have the largest fracture energy, splitting strength, and fracture work, while the specimens made by process D have the smallest value. Specially, the fracture energy of the specimens prepared by process C is 77.23% larger than that of the specimens prepared by process A, while the fracture energy of the specimens prepared by process D is 5.6% smaller than that of the specimens prepared by process A. The reason for this phenomenon is that the fiber is well dispersed in the specimens prepared by process C, which contributes to obtain a better crack resistance. For all CRAM specimens, with the increase of freeze–thaw cycles, splitting strength and fracture work of fiber CRAM decrease. However, there is an obvious difference in the reduction rate of splitting strength and fracture work, especially for the specimens under the water saturation condition. The specimens made by process C have the smallest reduction rate, which indicates a better resistance to freezing and thawing damage. According to the analysis of fiber macro-distribution state in loose CRAM, the fiber dispersion is affected by the humidity conditions in the mixing environment. The best humidity conditions are obtained for fiber dispersion in process C. Based on the SEM observation, the overlapping bridging network structure can be observed in the microstructure of the specimens prepared by process C, allowing the mixture to better transfer and disperse stress.

Keywords: cold recycled asphalt mixture; fiber mixing process; resistance to cracking; freeze–thaw damage; fiber dispersion state

check for updates

Citation: Wang, M.; Huo, T.; Xing, C.; Wang, Y. Influence of Fiber Mixing Process on the Cracking Resistance of Cold Recycled Asphalt Mixture. *Appl. Sci.* **2023**, *13*, 999. https://doi.org/10.3390/app13020999

Academic Editor: Luís Picado Santos

Received: 1 December 2022
Revised: 26 December 2022
Accepted: 3 January 2023
Published: 11 January 2023

Copyright: © 2023 by the authors. Licensee MDPI, Basel, Switzerland. This article is an open access article distributed under the terms and conditions of the Creative Commons Attribution (CC BY) license (https://creativecommons.org/licenses/by/4.0/).

1. Introduction

Cold recycled asphalt mixture (CRAM) is one of the most promising technologies to reduce carbon emissions in road construction due to many advantages, such as lower greenhouse gas emissions, economic cost effectiveness, and better working conditions for construction workers [1]. However, the performance of CRAM is not as good as that of traditional hot mix asphalt mixture [2]. In particular, it is very sensitive to cold climates or freeze–thaw environments due to its poor cracking resistance, insufficient early strength, and poor fatigue durability [3,4]. As a result, CRAM is generally used in the lower layers

of pavement structures, such as base course or underlayer of asphalt pavements [5]. It is necessary to take effective measures to enhance the performance of CRAM, so that it can be used in the place of hot mixture asphalt (HMA) under a certain condition.

Currently, fibers have been widely used to enhance the engineering properties because of its good reinforcement and toughening effect [6–12]. Specifically, fiber reinforcement improves fatigue life and retards rutting by increasing resistance to cracking and permanent deformation [13]. Wang et al. [14] explored the effect of four kinds of fibers on the mechanical properties of CRAM, and the results showed that basalt fibers had the most significant improvement on the fatigue properties. Keum et al. [15] found that polypropylene fibers could improve the bearing capacity and water damage resistance of emulsified asphalt mixture. Research conducted by Zeng et al. [16] reported that basalt fibers had an obvious effect on the splitting strength of asphalt mixture under low temperature conditions, and the reinforcing effect of fiber obviously played an important role in preventing cracks. Kong et al. [17] also confirmed that basalt fibers delayed the expansion of micro cracks of emulsified asphalt mixture. Nevertheless, Wang et al. [18] concluded that the addition of basalt fibers reduced the low temperature cracking resistance of CRAM. The reason for this phenomenon may be due to something wrong with the mixing process and the dosage of fiber in CRAM. The mixing process of the fibers directly affects the dispersion state of the fibers in CRAM, which determines the properties of CRAM to a certain extent. The research on fiber mixing processes may give a reasonable explanation for this phenomenon.

In addition, the fiber content and modification mechanisms of CRAM also received great attention. Jiang et al. [19] studied the effect of fiber content on the road performance of CRAM. It was found that various road performance indicators such as dynamic stability, flexural-tensile strain, and the freeze–thaw splitting strength of CRAM first increased and then decreased with the increase of fiber content. Therefore, it is very important to select the appropriate dosage of fibers for CRAM to meet the performance requirement of different service environments. Furthermore, scanning electron microscopy (SEM) has also been proven to be an effective means for the research of fiber modification mechanisms. It can be observed that fibers enhanced the integrity of CRAM through interfacial reinforcement [20].

Thus, the objective of this study is to evaluate of the influence of fiber mixing process on the cracking resistance of CRAM from multiple perspectives. To achieve this goal, four fiber mixing processes were designed by changing the addition order of fiber. Semicircle bending tests and indirect tensile tests were conducted to characterize the cracking behavior of CRAM at low temperature. Moreover, freeze–thaw cycle tests under both dry and water-saturated conditions were also designed to investigate the effect of fiber mixing process on the freeze–thaw damage behavior of CRAM. Finally, SEM was also used to analyze the effect of fiber mixing process on its micro dispersion in CRAM. The research results in this study provide basic data for the evaluation of anti-cracking performance of fiber CRAMs, and technical reference and theoretical support for the design of fiber mixing process in engineering practice.

2. CRAM and Fiber Mixing Process Design

2.1. Experimental Materials

2.1.1. Fibers

Considering that basalt fiber has good adsorption and anchoring effect on asphalt due to its high modulus and rough surface texture [17], the basalt fiber is selected in this study, as presented in Figure 1. The related properties of basalt fiber are shown in Table 1.

Table 1. The properties of basalt fiber.

Items	Diameter (μm)	Length (mm)	Melting Point (°C)	Density (g/cm^3)	Moisture Absorption (%)	Tensile Strength (MPa)	Elongation at Break (%)
Test results	16	6	1500	4.36	0.1	≥2000	2.7



Figure 1. Basalt fiber.

2.1.2. Emulsified Asphalt

Emulsified asphalt used in this study was self-made in the laboratory, and its basic performance indicators are shown in Table 2.

Table 2. Main technical indexes of emulsified asphalt.

Test Items		Unit	Test Results	Technical Requirements
Demulsification speed			slow crack	slow crack
Particle charge			cation	cation
Residue on sieve (1.18 mm)		%	0.02	≤0.1
Storage stability	1 d	%	0.5	≤1
	5 d	%	0.9	≤5

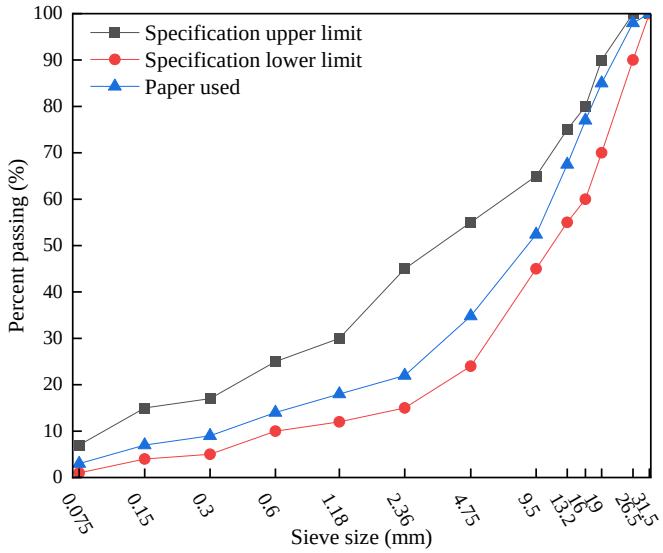


Figure 2. Final design gradation of CRAM.

2.1.3. RAP and Other Materials

Reclaimed asphalt pavement (RAP) materials used in this study were divided into three grades: 0–5 mm, 5–10 mm, and 10–30 mm. To obtain a good CRAM gradation, some diabase aggregates (10~20 mm) and limestone powder were also used. The final design gradation of CRAM is shown in Figure 2. Referring to the technical specifications for highway pavement recycling (JTG/T 5521-2019), the optimum water content and the optimum emulsified asphalt

content were 3.8% and 3.5%, respectively. In addition, ordinary portland cement was also added as an active additive, and the content of cement in CBM is 1.5%.

2.2. Fiber Content in CRAM and Fiber Mixing Process Design

2.2.1. Optimum Fiber Content

For the purpose of determining the optimum fiber content, CRAM with four fiber content (by mass of dry aggregates) of 0.1%, 0.2%, 0.3%, and 0.4% were prepared to explore the effect of fiber content on the performance using splitting strength tests at 15 °C and freeze–thaw splitting tests in accordance with the test code for asphalt and asphalt mixture in highway engineering (JTGE 20-2011) [21]. The test results of fiber CRAM are shown in Figure 3. With the increase of fiber content, the void of CRAM gradually increases, while the splitting strength and freeze–thaw splitting strength ratio increases first and then decreases. When the fiber content is 0.2%, the freeze–thaw splitting strength ratio and the splitting strength reach the maximum value, which can be attributed to the fact that when the fiber content is too large, fiber agglomeration occurs and thus has a negative impact on the performance of CRAM. In addition, a larger fiber content is not good for the compaction of the mixture, resulting in the void increase, as shown in Figure 3a. Therefore, based on these results, 0.2% fiber content by mass of dry aggregates was selected to prepare fiber CRAM in this study.

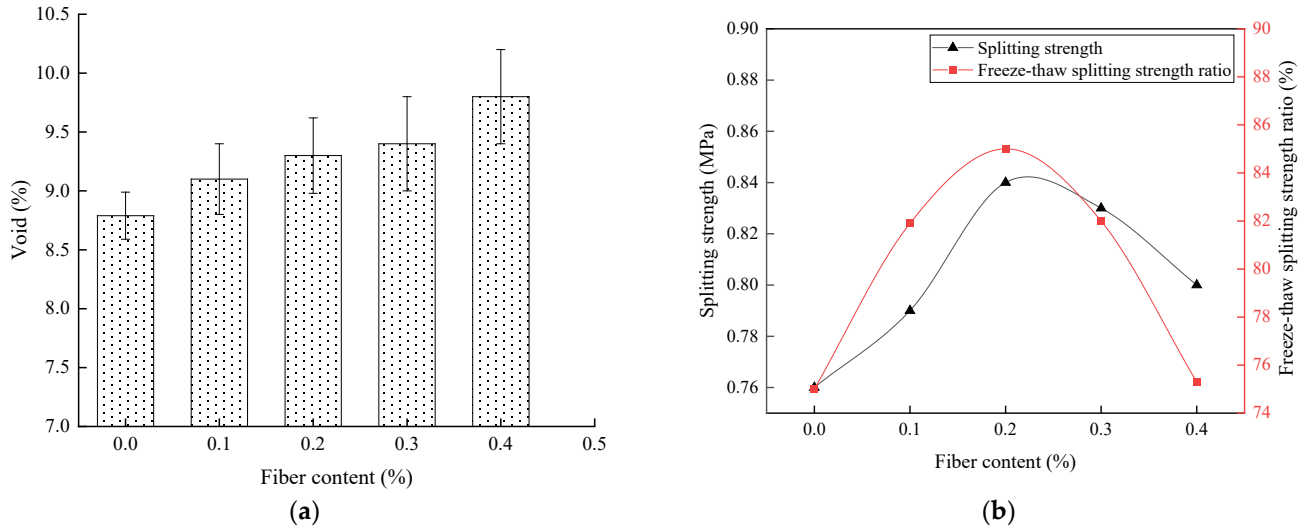


Figure 3. The effect of fiber content on the performance of CRAM: (**a**) void; (**b**) splitting strength and freeze–thaw splitting strength ratio.

2.2.2. Fiber Mixing Process Design

Under the condition that the total mixing time (t = 180 s) remains unchanged, four kinds of fiber mixing processes of CRAM were studied, which were named as process A, process B, process C, and process D, respectively. Among them, process A was selected as the control group because of no fiber incorporation. By contrast, in process B, the fiber and mineral aggregates were added to the mixing pot together. In process C, fiber was added to the mixing pot after adding water and before adding emulsified asphalt. In process D, fiber was added to the mixing pot after adding emulsified asphalt. The schematic of the specific mixing process is shown in Figure 4.

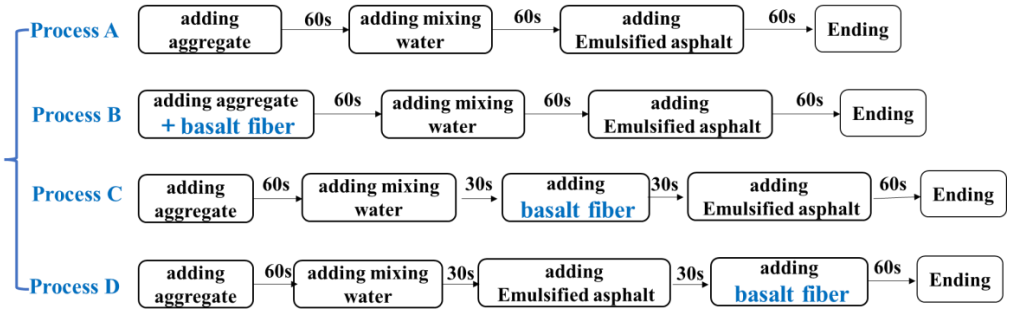


Figure 4. Four kinds of fiber mixing processes.

3. Experimental Methods

To evaluate the influence of fiber addition processes on the cracking performance of CRAM, indirect tensile tests, semicircle bending tests, freeze–thaw cycle tests, and scanning electron microscope tests were conducted to evaluate the performance of fiber CRAM prepared by different processes. The specific research method and test scheme are shown in Figure 5.

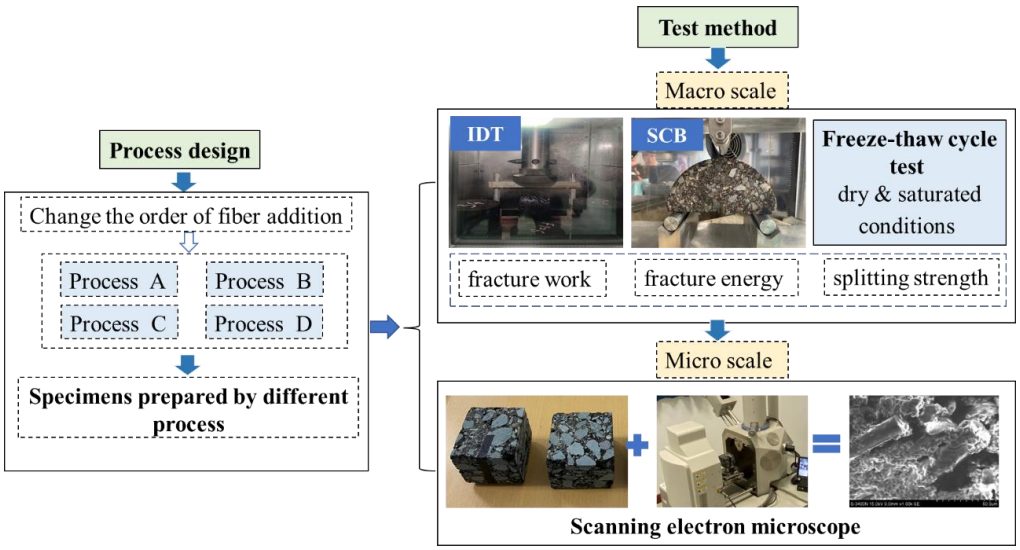


Figure 5. Test and research plan.

3.1. Crack Resistance Tests

3.1.1. Indirect Tensile Tests

The indirect tensile (IDT) test was carried out in accordance with the test code for asphalt and asphalt mixture in highway engineering (JTGE 20-2011) [21]. IDT specimens with the dimensions of φ 101.6 mm × 63.5 mm were prepared by the standard Marshall method. The test temperature was −10 °C, and the loading rate of the specimen was 1 mm/min. The test process and the load-displacement curves are shown in Figure 6. It is generally believed that the greater the fracture work (W) or splitting strength, the stronger the ability to resist low temperature cracking. Therefore, splitting strength and fracture work (*W*) were selected as evaluate indicators. The calculation diagram of fracture work is illustrated in Figure 6b, and the specific calculation method of fracture work is shown in Equation (1):

$$W = \int_0^L Pdl \tag{1}$$

where:

l—the deformation during the loading process of the specimen;

P—the load during the loading process of the specimen;
L—the deformation when the specimen load reaches the maximum.

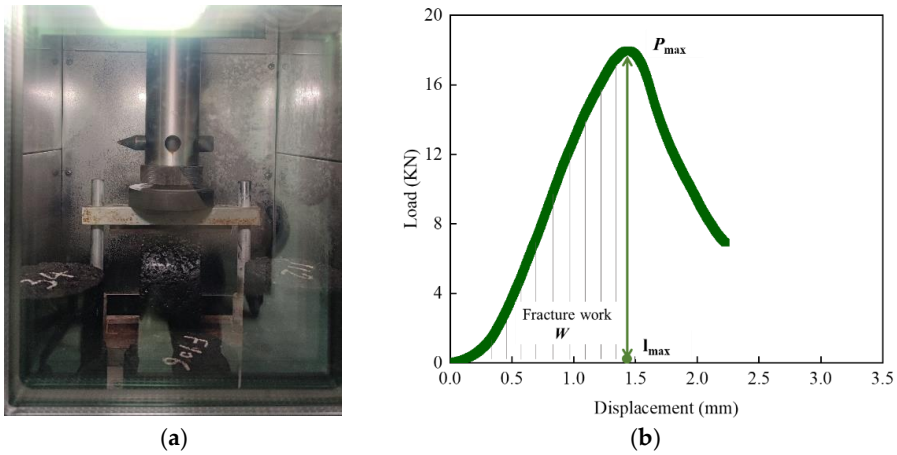


Figure 6. The process and loading curves of IDT test: (**a**) the test process; (**b**) the load-displacement curve.

3.1.2. Semicircle Bending Tests

Considering that the stress state of semicircle bending (SCB) test specimen is closer to that of the actual pavement [22], SCB tests can be used to evaluate the low-temperature anti-cracking performance of asphalt mixture [23]. According to the technical specification for cold recycling construction of emulsified asphalt on highway asphalt pavement (DB13/T-2020) [24], SCB test was conducted. The schematic of SCB test is shown in Figure 7. SCB specimens with a dimension of φ 152.4 mm × 105 mm were firstly prepared by large Marshall methods. Then the compacted specimen was cut by a high precision cutting machine into the SCB test specimen (as presented in Figure 7a) whose size diameter and thickness was 150 mm and 50 mm, respectively. The notch depth and width of semicircular specimen was 15 mm and 2.5 mm, respectively. During the test, the SCB test specimen was supported by two fixed rollers with a span of 120 mm (as presented in Figure 7c). The temperature of SCB test was −10 °C, the LLD control mode was used for loading, and the loading rate was 1 mm/min. The SCB loading curves is shown in Figure 7d.

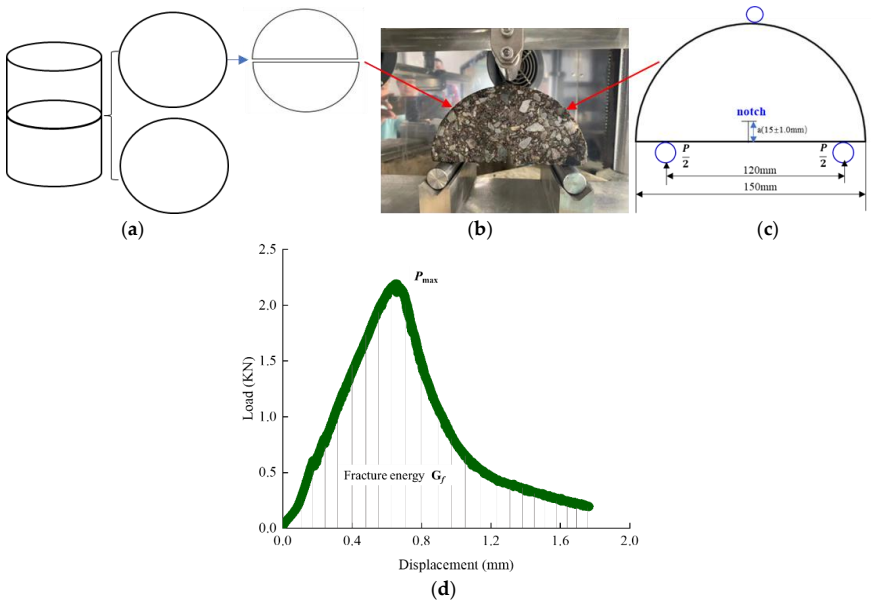


Figure 7. Semi-circular bending test schematic: (**a**) compacted specimens and test slices; (**b**) loading process; (**c**) key dimensions; (**d**) SCB loading curves and calculation diagram of fracture energy.

In the view of the evaluation index, fracture energy can be used to characterize the ability of CRAM to resist low-temperature cracking. Fracture energy (G_f) is defined as the work of SCB specimen generating unit area fracture surface, namely the ratio of force-displacement curve area to specimen fracture area, which could reflect the load and deformation of the specimen at each moment during the SCB test. The larger the fracture energy value, the better the resistance to cracking of asphalt mixture [25,26]. The calculation diagram of G_f is shown in Figure 6d and the calculation method is presented in Equation (2).

$$Gf = \frac{\int P d\mu}{(r-a)t} \quad (2)$$

where:

G_f—axial displacement fracture energy;
P—test tensile load;
μ—axial displacement;
r—radius of the specimen;
a—incision length;
t—specimen thickness.

3.2. Freeze–Thaw Cycle Tests

To evaluate the effect of fiber mixing process on the freeze–thaw damage behavior of CRAM, freeze–thaw cycle tests were carried out under both the dry and saturated conditions [27]. The specimens used for freeze–thaw cycle tests were also prepared by the Marshall method. The dimension of the specimen was 101.6 ± 0.25 mm and the height was 63.5 ± 1.3 mm, and all specimens were divided into two groups on average. A group of specimens were used for the saturation test. Based on the splitting strength and fracture work obtained from the indirect tensile test at the temperature of −10 °C, the freeze thaw damage behavior of CRAM was characterized.

3.2.1. Saturation Tests of Specimen

First, the specimen was put in a 60 °C blast oven for curing to constant weight. Then, the specimen was cooled at room temperature. Finally, the test specimen was placed under the vacuum conditions for 15 min. When the test specimen standing in water had a constant weight, the test specimen surface was dried with a wet towel to obtain the test specimen under the fully saturated test condition.

3.2.2. Freeze–Thaw Cycle Tests of Specimen

First, both the dry and saturated specimens were wrapped and sealed with plastic wrap, respectively. Then, the test specimens were placed in the refrigerator at –20 °C for 6 h. Finally, the test specimens were put in a constant temperature water bath at 60 °C for 4 h to complete one freeze–thaw cycle test. According to the above freeze–thaw cycle process, 3, 5, 10, and 20 freeze–thaw cycles tests were conducted.

3.3. Scanning Electron Microscope

To better understand asphalt or mixture, many new microanalysis techniques have been employed to provide an insight into the asphalt characteristics [26–31]. SEM is one of the electronic imaging techniques, and has some advantages in capturing the morphology of specimens because of its high resolution. SEM has been used successfully to observe the interface microstructure of mixtures [26,30,31]. In this study, to ensure the observation accuracy, the CRAM specimen was refined before the SEM test, as shown in Figure 8. First, the double-sided adhesive tape was sticked on the specimen table to fix the mixture specimen. Then, the observation area of the specimen was connected with the specimen table with conductive adhesive. Finally, a vacuum cleaner was used to remove impurities from the specimen.

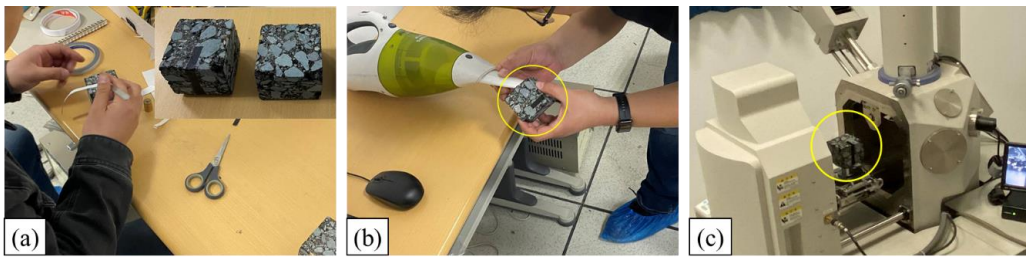


Figure 8. Fine processing of SEM test specimens: (**a**) specimen for pasting conductive adhesive; (**b**) removing impurities on the surface of the specimen; (**c**) the specimen placed in the observation chamber.

4. Results and Discussions

4.1. Resistance to Cracking

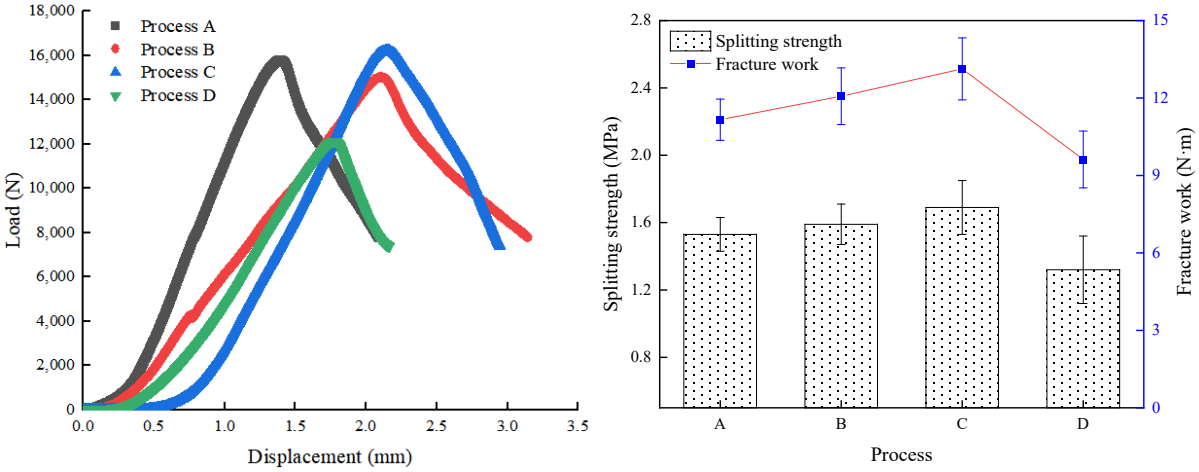
4.1.1. The Fracture of Indirect Tensile Tests

Based on the results of the IDT test, the load–displacement curve and the relationship between splitting strength, fracture work, and fiber mixing processes are shown in Figure 9. It was found that the fiber mixing process has significant effects on the fracture cures, splitting strength, and fracture work of IDT specimens. As presented in Figure 9a, the rise rate of the loading curves of the specimens prepared by process B, process C and process D were smaller than that of the specimen prepared by process A. In addition, the displacement value corresponding to peak load of the specimens prepared by process B, process C and process D were obviously larger than that of the specimens prepared by process A. This indicates that the fracture toughness of fiber CRAM is better than that of CRAM with no fiber. This phenomenon could be attributed to the fact that the fiber plays a role of reinforcement and bridge in the mixture. In addition, the modification effect of fiber on the CRAM is also strongly affected by the fiber mixing process. As illustrated in Figure 9b, for both the splitting strength index and the fracture work, the order of IDT specimens prepared by different processes is: process C > process B > process A > process D. The specimens made by process C have the largest splitting strength and fracture work, while the specimens made by process D have the smallest splitting strength and fracture work. As reported in the literature [18], the larger the splitting strength or fracture work, the better the resistance to cracking of the mixture. Furthermore, it is worth noting that the splitting strength of specimens made by process D is 13.72% smaller than that of specimens made by process A, and the fracture work is 13.80% smaller than that of specimens made by process A. The reason for this phenomenon is that the fiber is well dispersed in the specimens prepared by process C, which contributes to obtaining a better crack resistance. Thus, for the fiber CRAM with improper fiber mixing processes, the addition of fiber will not enhance the crack resistance, but will reduce the crack resistance of the mixture. The fiber mixing process selection is very important in engineering practice.

4.1.2. The Fracture Performance of SCB Test

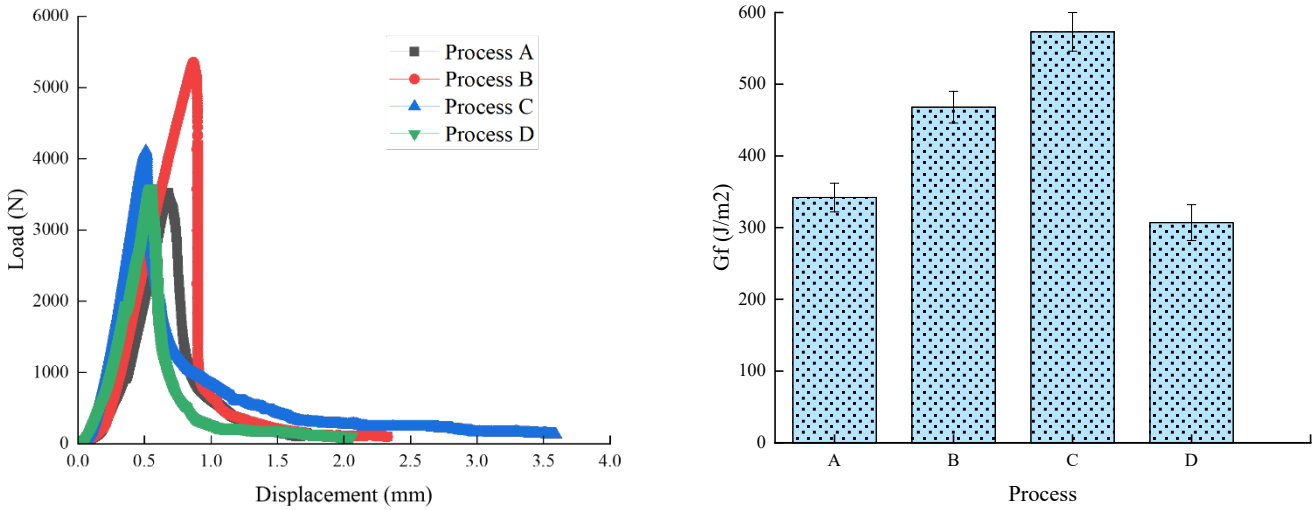
Based on the results of the SCB test, the load–displacement curve and the relationship between fracture energy and fiber mixing processes are shown in Figure 10. As shown in Figure 10, the fiber mixing process has also significant effects on the fracture curves and the fracture energy of SCB specimens. In the view of the fracture curves, both the peak load and maximum displacement of the specimen prepared by different processes present a certain difference. Overall, the fracture curves also show great similarity to the typical curve of the medium plastic material [23], which indicates that fiber CRAM has both elastic deformation and visco-plastic deformation, showing obvious stage characteristics from low deformation and cracking. Moreover, the SCB test is also based on the principle of energy theory. Given this, fracture energy was used to quantitatively evaluate the crack resistance of fiber CRAM in this study. The higher the fracture energy value, the better the fracture toughness of the asphalt mixture [24,25]. Based on the calculation results in

Figure 10b, the fracture energy of SCB specimens made by different processes are 325 J/m^2, 485 J/m^2, 576 J/m^2, and 307 J/m^2, respectively. The specimens prepared by process C have the largest fracture energy, while the specimens prepared by process D have the smallest fracture energy. Specifically, the fracture energy of the specimens prepared by process C is 77.23% larger than that of the specimens prepared by process A, while the fracture energy of the specimens prepared by process D is 5.6% smaller than that of the specimens prepared by process A. These findings are agreement with the results of IDT test.



(**a**) (**b**)

Figure 9. Results of indirect tensile test: (**a**) load–displacement curves; (**b**) fiber mixing processes and splitting strength or fracture work.



(**a**) (**b**)

Figure 10. Results of SCB test: (**a**) load–displacement curves; (**b**) fiber mixing processes and fracture energy.

To further characterize the correlation of test results, the correlation between the fracture energy and fracture work were analyzed, as shown in Figure 11. It was found that there is a good linear correlation between the two test results. Therefore, based on the results, process C is recommended for fiber CRAM. Nevertheless, the process D does not enhance the crack resistance of the CRAM. Maybe the reason for this phenomenon is that there is something wrong with the fiber dispersion states in the CRAM. In contrast, process C can make the fiber obtain the best dispersion state in CRAM, resulting in the addition of fiber greatly contributing to improving the crack resistance of CRAM.

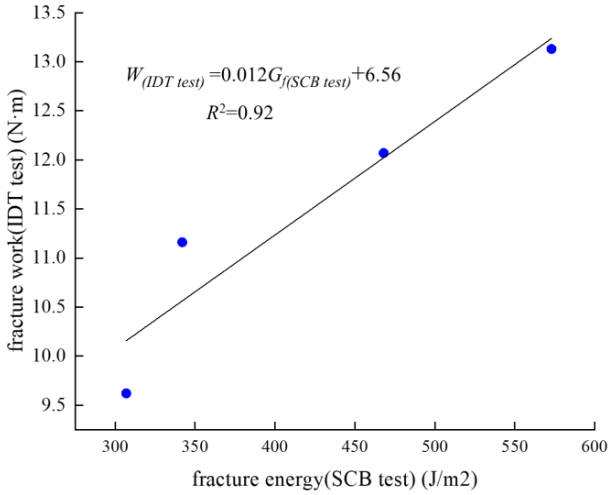


Figure 11. The correlation between fracture energy and fracture work.

4.2. Resistance to Freeze–Thaw Damage

Given that there was a good correlation of the results between SCB tests and ID tests, only the ID test was carried out to study the influence of fiber mixing process on the freeze–thaw damage performance of CRAM. At the same time, to reduce the experimental amount, only the samples of three processes (process A, process C and process D) were tested. Based on the results of freeze–thaw cycle test, the relationship between splitting strength and freeze–thaw cycles of fiber CRAM is illustrated in Figure 12, and the relationship between fracture work and freeze–thaw cycles of fiber CRAM is shown in Figure 13. It can be seen that with the increase of freeze–thaw cycles, the splitting strength and fracture work of fiber CRAM decrease. The fiber mixing process has a significance effect on the reduction rate of splitting strength and fracture work, especially for the specimens under the water saturation condition. After 20 freeze–thaw cycles under completely dry test conditions, the splitting strength of CRAM prepared by process A decreased by 21.6%, while that of fiber CRAM prepared by process C and process D decreased by 9.47% and 20.45%, respectively. Similarly, after 20 freeze–thaw cycles under water saturation condition, the splitting strength of CRAM prepared by process A decreased by 57.52%, while that of fiber CRAM prepared by process C and process D decreased by 34.91% and 39.39%, respectively. Therefore, from the analysis of splitting strength, the fiber CRAM made by process C has the smallest reduction rate, which indicates that the best fiber mixing process is process C.

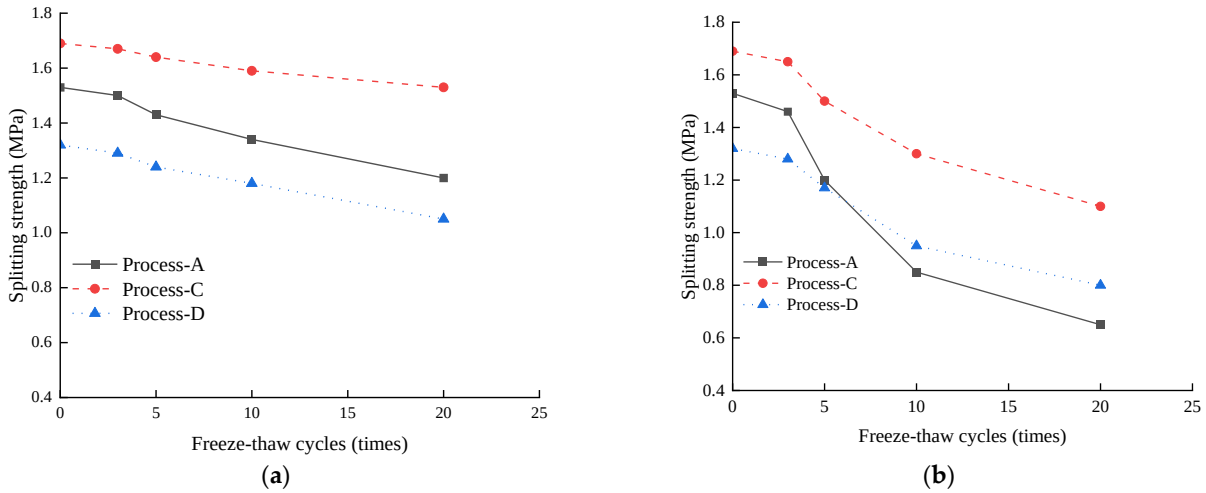


Figure 12. Relationship between splitting strength and freeze–thaw cycles: (**a**) completely dry condition; (**b**) water saturation condition.

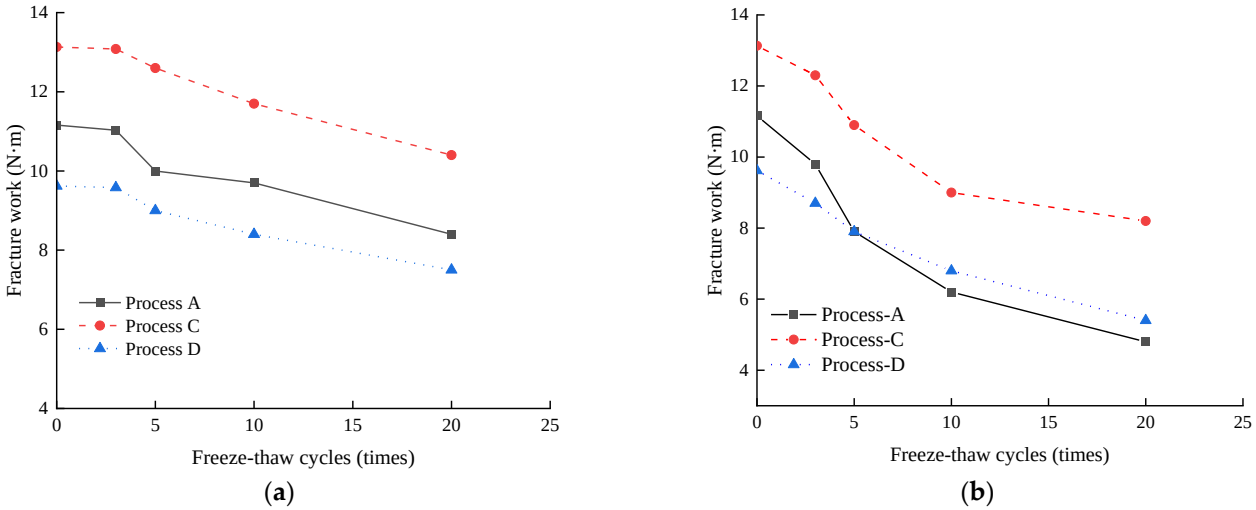


Figure 13. Relationship between fracture work and freeze–thaw cycles: (**a**) completely dry condition; (**b**) water saturation condition.

On the other hand, from the analysis of fracture work in Figure 13, after 20 freeze–thaw cycles under completely dry test conditions, the fracture work of CRAM prepared by process A decreased by 24.73%, while that of fiber CRAM prepared by process C and process D decreased by 20.79% and 22.04%, respectively. Similarly, after 20 freeze–thaw cycles under water saturation condition, the fracture work of CRAM prepared by process A decreased by 56.99%, while that of fiber CRAM prepared by process C and process D decreased by 37.55% and 43.87%, respectively. The fiber mixture made by process C also has the smallest reduction rate of fracture work, while the CRAM made by process A has the largest reduction rate of fracture work. This is agreement with the analysis result of splitting strength. The greater the reduction rate of fracture work, the worse the freeze–thaw damage resistance of the fiber CRAM. Therefore, the fiber CRAM made by process C has the best resistance to freezing and thawing damage. This indicates that the fiber indeed improves the performance of CRAM against freeze–thaw damage and the proper fiber mixing process further enhances the effect of fiber modification.

4.3. Dispersion State of Fiber in the CRAM

4.3.1. Macro-Distribution State of Fiber in Loose CRAM

Based on the above analysis, the influence of fiber mixing process on the crack resistance of CRAM is obvious. It is necessary to further explore the dispersion state of fibers in CRAM. Figure 14 shows the fiber macro-distribution state in loose CRAM prepared by different processes after mixing. As presented in Figure 14, the influence of mixing process on fiber dispersion state in CRAM is significant. Such differences are mainly manifested in the surface coating state of the aggregate and the uniformity of fiber dispersion. We found that the surface coating state of aggregate is more sufficient and the uniformity of fiber dispersion is also better for the specimen prepared by process C. However, for the specimen prepared by process D, the fiber agglomeration phenomenon can be found. Furthermore, similar phenomena can be observed in the specimen prepared by process B. This is because that the dispersion state of fiber is affected by the humidity conditions in the mixing environment. For the CRAM made by process B, because of the lower humidity in the mixing environment, the dispersion resistance of fibers is higher, while for the CRAM made by process D, due to the excessive humidity, the fibers are agglomerated, resulting in the poor dispersion uniformity of fiber. In contrast, the best humidity condition is obtained for fiber dispersion in process C. It can be speculated that the dispersion state of fiber is closely related to the interfacial properties of the CRAM. Therefore, it is necessary to further explore the influence of fiber mixing process on micro-distribution state of fiber in CRAM.

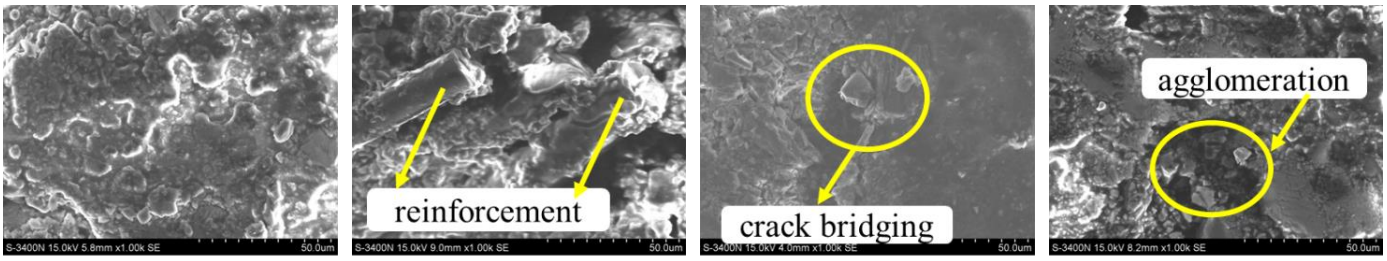


(**a**) (**b**) (**c**) (**d**)

Figure 14. Fiber macro-distribution state in loose CRAM: (**a**) process A; (**b**) process B; (**c**) process C; (**d**) process D.

4.3.2. Micro-Distribution State of Fiber in CRAM Specimens

The fiber micro-distribution state in the CRAM specimen was obtained using scanning electron microscope technology, as shown in Figure 15. It was found that the internal microstructure of the CRAM without fiber is relatively loose, while the overlapping microstructure of fibers is observed in fiber CRAM. As a result of a reinforcing role of fiber, the addition of fiber can enhance the fracture toughness of the mixture. However, because of the difference in fiber micro-distribution state, the toughness against cracking is also different. Due to the fiber agglomeration phenomenon in Figure 15b,d, the micro dispersion state of fiber is poor, which reduces the uniformity of fiber in CRAM. In contrast, an overlapping bridging network structure can be observed in Figure 15c, which makes the fiber CRAM transfer and disperse stress better when it is stressed. In addition, this structure allows the fiber to pass through the microcrack and weak interface of the mixture, and the weak position of the interface can be strengthened by the bridging principle, so as to make up for the weak point of the aggregate adhesion in RAP. This finding is highly consistent with the literature [26]. Therefore, uniformly dispersed fibers can optimize the internal structure of the fiber mixture and enhance its ability to resist cracking.



(**a**) (**b**) (**c**) (**d**)

Figure 15. Microstructure of fiber in CRAM: (**a**) process A; (**b**) process B; (**c**) process C; (**d**) process D.

5. Conclusions

Four kinds of fiber mixing processes named A, B, C, and D were designed by changing the order of fiber addition. The effect of fiber mixing process on the cracking resistance of CRAM has been evaluated from multiple perspectives in this research. The main findings are concluded as follows:

(1) Based on the results of the semicircle bending test and indirect tensile test, fiber mixing processes have a significant effect on the cracking resistance of CRAM. The CRAM specimens prepared by process C have the largest fracture energy, splitting strength, and fracture work, while the specimens made by process D have the smallest value.

(2) For all CRAM specimens, with the increase of freeze–thaw cycles, splitting strength and fracture work of fiber CRAM decrease. However, there is an obvious difference in the reduction rate of splitting strength and fracture work, especially for the specimens under water saturation condition. The specimens made by process C have the smallest reduction rate, which indicates a better resistance to freezing and thawing damage.

(3) According to the analysis of fiber macro-distribution state in loose CRAM, the dispersion state of the fiber is affected by the humidity condition in the mixing environment. In contrast, the best humidity conditions are obtained for fiber dispersion in process C.
(4) Based on the SEM observation, an overlapping bridging network structure can be observed in the microstructure of the specimens prepared by process C, which means the mixture could transfer and disperse stress better when it is stressed. This reveals the mechanism of the influence of fiber mixing process on the resistance to cracking of CRAM from the micro level.

Based on the above results, it is critical to select the appropriate fiber mixing process for the CRAM in engineering practices. Moreover, the influence of the fiber mixing process on the fatigue performance of CRAM needs to be further verified. For this issue, we will study and discuss it in further study.

Author Contributions: Conceptualization: M.W. and C.X.; methodology, M.W.; investigation, T.H. and Y.W.; data curation, T.H.; writing—original draft preparation, M.W.; writing—review and editing, C.X.; funding acquisition, M.W. All authors have read and agreed to the published version of the manuscript.

Funding: The authors gratefully acknowledge the financial support obtained from the Gansu Provincial Science and Technology Plan Project (major science and technology projects) (Project No. 21ZD8JA003) and the Fundamental Research Funds for Central Universities (Project No. 3122018C018) of Civil Aviation University of China.

Institutional Review Board Statement: Not applicable.

Informed Consent Statement: Not applicable.

Data Availability Statement: The data presented in this study are available on request from the corresponding author. The data are not publicly available due to requirements of the funder.

Conflicts of Interest: The authors declare that they have no known competing financial interest or personal relationship that could have appeared to influence the work reported in this paper.

References

1. Jain, S.; Singh, B. Cold mix asphalt: An overview. *J. Clean. Prod.* **2021**, *280*, 124378. [CrossRef]
2. Yin, P.; Pan, B. Effect of RAP content on fatigue performance of hot-mixed recycled asphalt mixture. *Constr. Build. Mater.* **2022**, *328*, 127077. [CrossRef]
3. Zou, G.; Zhang, J.; Li, Y.; Lin, Z. Quantitative characterize binder blending and diffusion in recycled asphalt mixture: An environmental-friendly solution using wooden cube and 3D fluorescence image technology. *J. Clean. Prod.* **2021**, *293*, 126204. [CrossRef]
4. Wu, J.; Niu, Z.; Chen, H. Effect of aging on low-temperature crack resistance and water stability of polyester fiber asphalt mixture. *Mater. Res. Express* **2022**, *9*, 015101. [CrossRef]
5. Krasowski, J.; Buczyński, P.; Iwański, M. The Effect of Polymer Powder on the Cracking of the Subbase Layer Composed of Cold Recycled Bitumen Emulsion Mixtures. *Materials* **2021**, *14*, 5867. [CrossRef]
6. Rizwan, A.K.; Rahul, S. Strength and Durability Characteristics of Rice Husk Ash Concrete Reinforced with Polypropylene Fibres. *J. Civ. Eng.* **2018**, *12*, 653–668.
7. Xu, Q.; Chen, H.; Prozzi, J.A. Performance of fiber reinforced asphalt concrete under environmental temperature and water effects. *Constr. Build. Mater.* **2010**, *24*, 2003–2010. [CrossRef]
8. Tian, T.; Jiang, Y.; Yi, Y.; Fan, J.; Yang, D.; Deng, C. Fiber-Emulsified Asphalt Cold-Recycled Mixture Produced Using Vertical Vibration Compaction: Performance Study. *J. Mater. Civ. Eng.* **2022**, *34*, 04022114. [CrossRef]
9. Hui, Y.; Men, G.; Xiao, P.; Tang, Q.; Han, F.; Kang, A.; Wu, Z. Recent Advances in Basalt Fiber Reinforced Asphalt Mixture for Pavement Applications. *Materials* **2022**, *15*, 6826. [CrossRef]
10. Zhang, J.; Zheng, M.; Pei, J.; Zhang, J.; Li, R. Research on low temperature performance of emulsified asphalt cold recycled mixture and improvement measures based on fracture energy. *Materials* **2020**, *13*, 3176. [CrossRef]
11. Zhang, Q.; Hou, D.H.; Shi, J.C.; Shang, B.; Liu, T.B. Study on performance optimization of emulsified asphalt cold recycled mixture with mixed waste fibers. *Silic. Bull.* **2020**, *39*, 2662–2671.
12. Shanbara, H.K.; Ruddock, F.; Atherton, W. A laboratory study of high-performance cold mix asphalt mixtures reinforced with natural and synthetic fibres. *Constr. Build. Mater.* **2018**, *172*, 166–175. [CrossRef]
13. Abtahi, S.M.; Sheikhzadeh, M.; Hejazi, S.M. Fiber-reinforced asphalt-concrete–a review. *Constr. Build. Mater.* **2010**, *24*, 871–877. [CrossRef]

14. Wang, E.; Zhang, Q.Z. Effect of fiber on performance of emulsified asphalt cold recycled mixture. *New Build. Mater.* **2020**, *47*, 74–78.
15. Rhee, S.K.; Park, K.W. A study on Mechanical Characteristics of fiber modified emulsified asphalt mixture as environmentally-friend paving material. *Int. J. Highw. Eng.* **2006**, *8*, 23–30.
16. Zeng, S.H.; Dong, Y.; Xu, W.J. Experimental study on splitting of basalt fiber asphalt mixture. *New Build. Mater.* **2019**, *46*, 46–49.
17. Kong, L.; Lu, Z.; He, Z.; Shen, Z.; Xu, H.; Yang, K.; Yu, L. Characterization of crack resistance mechanism of fiber modified emulsified asphalt cold recycling mixture based on acoustic emission parameters. *Constr. Build. Mater.* **2022**, *327*, 126939. [CrossRef]
18. Wang, D.C.; Hao, P.W.; Lui, R.X.; Liu, N. Experimental study on low temperature crack resistance of emulsified asphalt cold recycled asphalt mixture. *J. Wuhan Univ. Technol.* **2020**, *44*, 64–68.
19. Jiang, Y.J.; Wang, R.X.; Liu, P.; Chen, Z.J. Effect of fiber on road performance of emulsified asphalt cold recycled mixture. *J. Dalian Univ. Technol.* **2020**, *60*, 62–68.
20. Wang, Z.G. Analysis on road performance and mechanism of emulsified asphalt cold recycled mixture mixed with fiber. *Highw. Eng.* **2016**, *41*, 262–266+288.
21. *Standard Test Methods of Bitumen and Bituminous Mixtures for Highway Engineering*; People's Communications Press: Beijing, China, 2011. (In Chinese)
22. Jahanbakhsh, H.; Hosseini, P.; Nejad, F.M.; Habibi, M. Intermediate temperature fracture resistance evaluation of cement emulsified asphalt mortar. *Constr. Build. Mater.* **2019**, *197*, 1–11. [CrossRef]
23. Wu, S.; He, R.; Chen, H.; Luo, Y. Low temperature characteristics of asphalt mixture based on the semi-circular bend and thermal stress restrained specimen test in alpine cold regions. *Constr. Build. Mater.* **2021**, *311*, 125300. [CrossRef]
24. Hebei Bureau of Quality and Technical Supervision. *Technical Specification for Cold Recycling of Emulsified Asphalt for Highway Asphalt Pavement*; People's Communications Press: Beijing, China, 2020.
25. Lv, S.S. Study on low temperature performance evaluation index of asphalt mixture based on bending test at low temperature. In *Applied Mechanics and Materials*; Trans Tech Publications Ltd.: Wollerau, Switzerland, 2012; Volume 193, pp. 427–430.
26. Li, Z.; Shen, A.; Wang, H.; Guo, Y.; Wu, H. Effect of basalt fiber on the low-temperature performance of an asphalt mixture in a heavily frozen area. *Constr. Build. Mater.* **2020**, *253*, 119080. [CrossRef]
27. Wang, T.; Chen, Y.; Zhu, C.; Liu, H.; Ma, C.; Wang, X.; Qu, R. High-and low-temperature fracture behavior of pervious asphalt mixtures under different freeze–thaw cycles based on acoustic emission technique. *Arab. J. Geosci.* **2022**, *15*, 1–15. [CrossRef]
28. Xing, C.; Liu, L.; Cui, Y.; Ding, D. Analysis of base bitumen chemical composition and aging behaviors via atomic force microscopy-based infrared spectroscopy. *Fuel* **2020**, *264*, 116845. [CrossRef]
29. Xing, C.; Jiang, W.; Li, M.; Wang, M.; Xiao, J.; Xu, Z. Application of atomic force microscopy in bitumen materials at the nanoscale, A review. *Constr. Build. Mater.* **2022**, *342*, 128059. [CrossRef]
30. Monich, P.R.; Berti, F.V.; Porto, L.M.; Henriques, B.; de Oliveira, A.P.N.; Fredel, M.C.; Souza, J.C. Physicochemical and biological assessment of PEEK composites embedding natural amorphous silica fibers for biomedical applications. *Mater. Sci. Eng. C* **2017**, *79*, 354–362. [CrossRef]
31. Maache, M.; Bezazi, A.; Amroune, S.; Scarpa, F.; Dufresne, A. Characterization of a novel natural cellulosic fiber from *Juncus effusus* L. *Carbohydr. Polym.* **2017**, *171*, 163–172. [CrossRef]

Disclaimer/Publisher's Note: The statements, opinions and data contained in all publications are solely those of the individual author(s) and contributor(s) and not of MDPI and/or the editor(s). MDPI and/or the editor(s) disclaim responsibility for any injury to people or property resulting from any ideas, methods, instructions or products referred to in the content.